BIOTECHNOLOGY

Multiple rereads of single proteins at single–amino acid resolution using nanopores

Henry Brinkerhoff[1], Albert S. W. Kang[1], Jingqian Liu[2], Aleksei Aksimentiev[2], Cees Dekker[1]*

A proteomics tool capable of identifying single proteins would be important for cell biology research and applications. Here, we demonstrate a nanopore-based single-molecule peptide reader sensitive to single–amino acid substitutions within individual peptides. A DNA-peptide conjugate was pulled through the biological nanopore MspA by the DNA helicase Hel308. Reading the ion current signal through the nanopore enabled discrimination of single–amino acid substitutions in single reads. Molecular dynamics simulations showed these signals to result from size exclusion and pore binding. We also demonstrate the capability to "rewind" peptide reads, obtaining numerous independent reads of the same molecule, yielding an error rate of $<10^{-6}$ in single amino acid variant identification. These proof-of-concept experiments constitute a promising basis for the development of a single-molecule protein fingerprinting and analysis technology.

Genetic sequence is a key source of information about protein primary sequence. However, because they do not directly encode information about protein abundance or about posttranslational modification and splicing of proteins, neither the DNA genome nor the RNA transcriptome fully describe the protein phenotype. A robust method for directly identifying proteins and detecting posttranslational modifications at the single-molecule level would greatly benefit proteomics research (*1*), enabling quantification of low-abundance proteins as well as distributions and correlations of posttranslational modifications, all at a single-cell level. Here, we provide proof-of-concept data for a nanopore-based approach that can discriminate single peptides at single–amino acid sensitivity with high fidelity and potential for high throughput. Although it is not presently capable of de novo protein sequencing, this nanopore peptide reader provides site-specific information about the peptide's primary sequence that may find applications in single-molecule protein fingerprinting and variant identification.

Recently, biological nanopores have been used as the basis of a single-molecule DNA sequencing technology (*2*) that is capable of long reads and detection of epigenetic markers in a portable platform with minimal cost (*3*). In such experiments, single-stranded DNA (ssDNA) is slowly moved step by step through a protein nanopore embedded in a thin membrane, partially blocking an electrical current carried by ions through the nanopore. The DNA stepping is accomplished using a DNA-translocating motor enzyme that moves DNA through the pore in discrete steps, yielding a series of steps in the ion current. Each ion current level characterizes the bases residing in the pore at that step, and the sequence of levels can be decoded into the DNA base sequence.

It has been hypothesized that nanopores can also be used for protein fingerprinting or sequencing (*4*, *5*). Methods in which small peptide fragments freely translocate through a pore have shown sensitivity to single amino acids (*6*–*8*), but we lack a method for determining the order of amino acids and reconstructing the sequence of single proteins. Using a ClpX protein unfoldase to pull a peptide through a nanopore yielded signals that effectively distinguished between different peptides (*9*), but these reads were difficult to interpret, in part because of the irregular stepping behavior of ClpX (*10*). In our study, we instead applied the precise stepwise control of a DNA-translocating motor (*11*–*13*) to pull a peptide through a nanopore, similarly to simultaneous work by Yan *et al.* (*14*) but presenting several key advances: the use of a helicase that pulls the polymer through MspA in smaller, half-nucleotide steps; the ability to identify single amino acid substitutions; and the capability to obtain high-fidelity signals by rereading the same single molecule multiple times.

We developed a system in which a DNA-peptide conjugate was pulled through a biological nanopore by a helicase that was walking on the DNA section (Fig. 1). The conjugate strand consisted of an 80-nucleotide DNA strand that was covalently linked to a 26–amino acid synthetic peptide by a DBCO click linker on the 5′ end of the DNA connecting to an azide modification at the C terminus of the peptide (materials and methods section 1 and fig. S1). A negatively charged peptide sequence of mostly aspartic acid (D) and glutamic acid (E) residues was chosen so that the electrophoretic force assisted in pulling the peptide into the pore. We used the mutant nanopore M2 MspA (*15*) with a cuplike shape that separates the helicase by ~10 nm from the constriction of the pore where the blockage of ion current occurs (*16*). For the DNA-translocating motor enzyme, we used Hel308 DNA helicase because (i) it pulls ssDNA through MspA in half-nucleotide ~0.33-nm observable steps (*13*), which are close to single–amino acid steps; (ii) because it is a stable and processive helicase that tolerates high salt concentrations (*16*); and (iii) its >50 pN pulling force (*16*) is likely to denature any secondary structure in target peptides.

We found that, similar to nanopore reads of DNA, ratcheting a peptide through the nanopore generated a distinct steplike pattern in the ion current (Fig. 1D). Durations of ion current steps varied from read to read, but the sequence of levels was highly reproducible (fig. S2). The progression of ion current steps was accurately identified using custom software (materials and methods section 2 and fig. S3), and further analysis was performed on the sequence of the median ion current values for each step (Fig. 1E).

This sequence of ion current levels first closely tracked the sequence expected for the template strand of DNA, which can be predicted using a DNA sequence–to–ion current map developed previously (*17*, *18*) (materials and methods section 3). After the end of the DNA crossed to the cis side of MspA's constriction, we continued to observe stepping over the linker (a length of ~2 nm, or six Hel308 steps), and subsequently over the peptide. The stepping of the peptide through the MspA constriction produced distinguishable ion current steps, much like those from DNA, but with a higher average ion current. Because individual reads might contain a varying number of steps owing to helicase backstepping and errors in step segmentation, we identified these features by cross-comparison of several independent reads, producing a "consensus" ion current sequence free of helicase missteps or step-segmentation errors (materials and methods section 4). By counting the steps in these consensus sequence traces, we determined the parts of the traces that corresponded to the linker (the first six steps after the DNA) and the peptide (all steps thereafter) in the MspA constriction. We confirmed this analysis by altering the peptide sequence at a selected site and observing the location of the resulting change in the ion current stepping sequence, as discussed below. We restricted further analysis to reads containing both DNA and peptide sections (materials and methods section 5 and fig. S4).

Our approach allowed us to discriminate peptide variants that differed by only a single amino acid. We obtained reads (N = 211) of three different DNA-peptide conjugates in 19

[1]Department of Bionanoscience, Kavli Institute of Nanoscience, Delft University of Technology, 2629 HZ Delft, Netherlands. [2]Center for Biophysics and Quantitative Biology and Department of Physics, University of Illinois at Urbana-Champaign, Urbana, IL 61801, USA.
*Corresponding author. Email: c.dekker@tudelft.nl

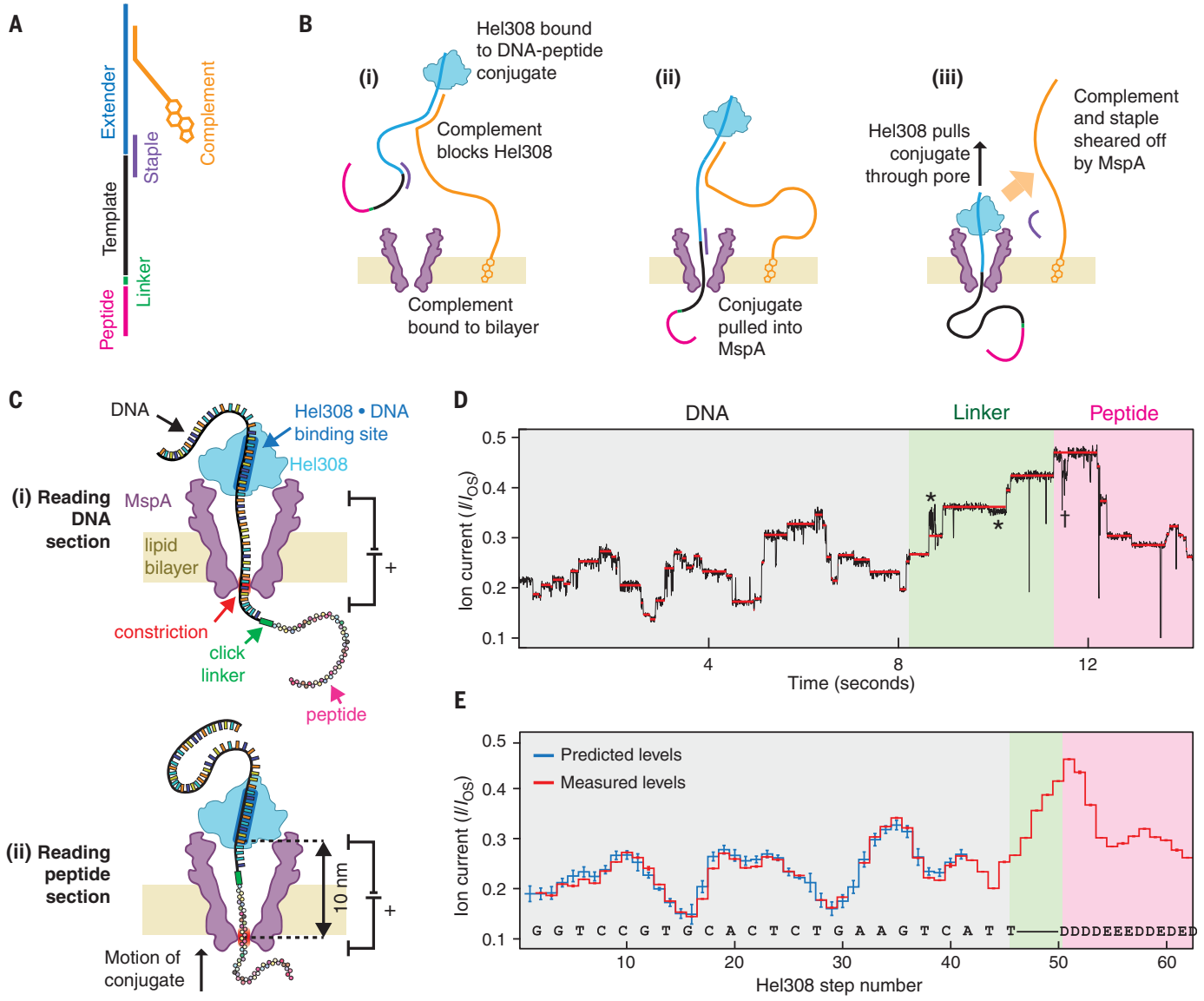

Fig. 1. Reading peptides with a nanopore. (**A**) The DNA-peptide conjugate consists of a peptide (pink) attached via a click linker (green) to an ssDNA strand (black). This DNA-peptide conjugate is extended with a typical nanopore adaptor comprised of an extender that acts as a site for helicase loading (blue) and a complementary oligo with a 3′ cholesterol modification (gold). (**B**) The cholesterol associates with the bilayer as shown in (i), increasing the concentration of analyte near the pore. The complementary oligo blocks the helicase, until it is pulled into the pore (ii), causing the complementary strand to be sheared off (iii), whereupon the helicase starts to step along DNA. (**C**) As the helicase walks along the DNA, it pulls it up through the pore, resulting in (i) a read of the DNA portion followed by (ii) a read of the attached peptide. (**D**) Typical nanopore read of a DNA-peptide conjugate (black), displaying steplike ion currents (identified in red). The asterisks indicate a spurious level not observed in most reads and therefore omitted from further analysis. The dagger symbol indicates a helicase backstep. The ion current is displayed as a fraction of the open pore current I_{OS}. (**E**) Consensus sequence of ion current steps (red), which for the DNA section is closely matched by the predicted DNA sequence (blue). The linker and peptide sections are identified by counting half-nucleotide steps over the known structural length of the linker. Error bars in the measured ion current levels are errors in the mean value, often too small to see. Error bars in the prediction are standard deviations of the ion current levels that were used to build the predictive map in previous work (*18*).

different pores, where the peptide sequences consisted of a mixture of negatively charged D and E residues, with a single variation—that is, D, glycine (G), or tryptophan (W)—placed four amino acids away from the C terminus that connected to the linker (see table S1 for full sequences). The three variants showed a reproducible difference at the site of the substituted amino acid, which could be seen by comparing the consensus sequences of ion current levels (Fig. 2, A and B). As is typical of nanopore experiments, a single-site variation was found to affect several ion current steps, because an "8-mer" of amino acids around the pore constriction of MspA affects the ion current blockage level (*11*, *17*) owing to the finite constriction height and stochastic displacements of the strand up and down through the nanopore (*19*). The center of the differing region in the ion current sequence was at the expected site: ~10 helicase steps away from the end of the DNA section (six half-nucleotide steps for the linker and four more along the peptide to the variant site). The signals varied by several standard deviations over multiple sequential levels, demonstrating that variations as small as a single amino acid substitution

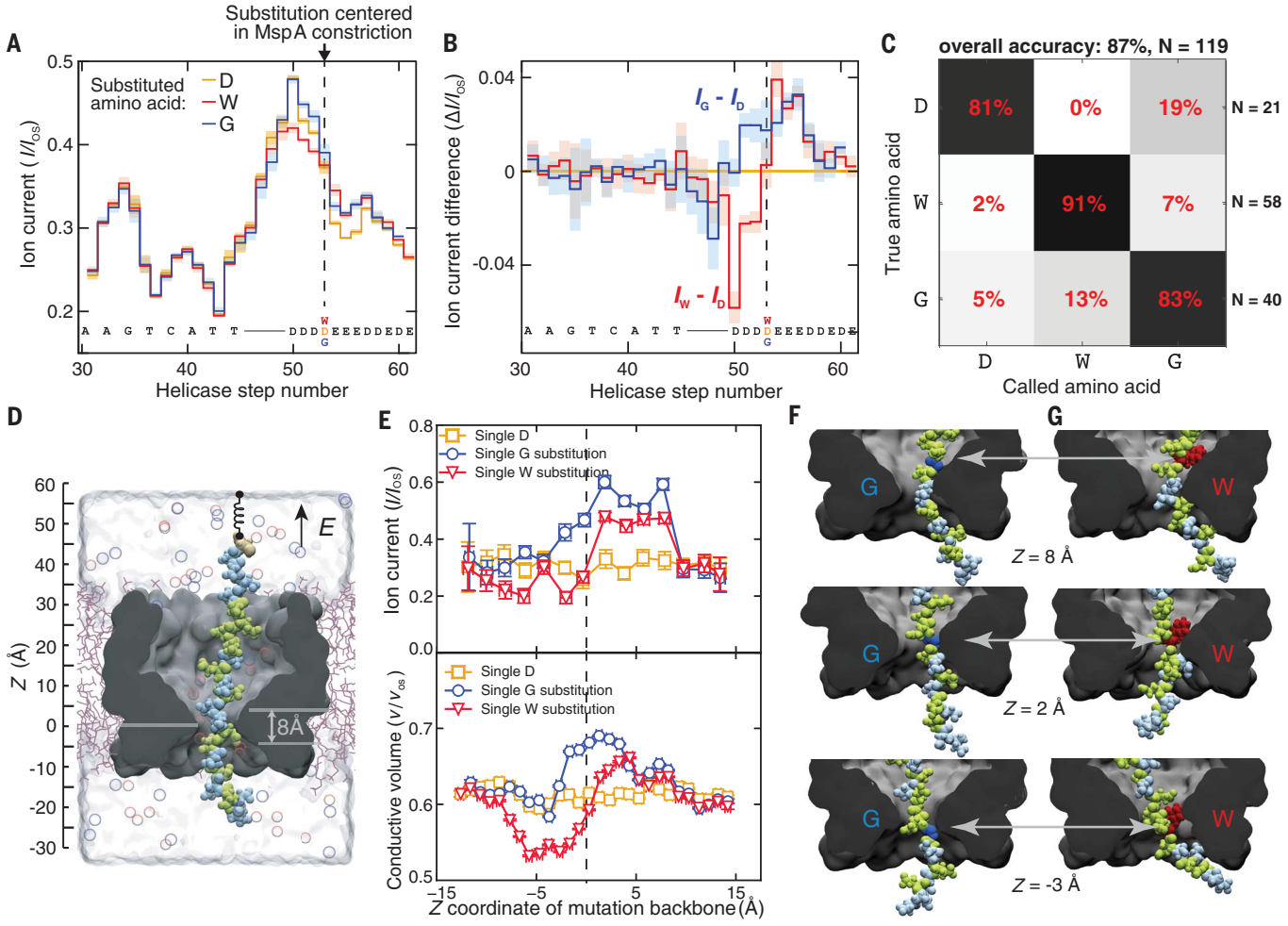

Fig. 2. Detection of single amino acid substitutions in single peptides. (**A**) Consensus ion current sequences for each of the three measured variants (D, gold; W, red; G, blue), which differ significantly at the site of the amino acid substitution. (**B**) Difference in ion current between the W (red) and G (blue) variants and the D variant. Error bars are standard deviations. (**C**) Confusion matrix showing error modes of a blind classifier in identifying variants of reads, demonstrating an 87% single-read accuracy. (**D**) All-atom model where a reduced-length MspA pore (gray) confines a polypeptide chain (Glu, green; Asp, light blue; Cys, beige). The top end of the peptide is anchored using a harmonic spring potential, representing the action of the helicase at the rim of a full-length MspA. Water and ions are shown as semitransparent surface and spheres, respectively. (**E**) (Top) Ionic current in MspA constriction versus *z* coordinate of the mutated residue backbone from MD simulations. (Bottom) Fraction of nanopore construction volume available for ion transport. Vertical and horizontal error bars denote standard errors and standard deviations, respectively. (**F** and **G**) Representative molecular configurations observed in MD simulations of peptide variants. Glycine and tryptophan residues are shown in dark blue and red, respectively. Considerable peptide–pore surface interactions are observed.

could be resolved. The differences of the ion currents for the W- and G-substituted variants from the D-substituted variant (Fig. 2B) showed a notable behavior: when G, which has just a hydrogen atom as a side chain, occupied the nanopore constriction, we saw higher ion current levels, as expected from a smaller amino acid volume. But when the bulky W variant moved through the constriction, the ion current first decreased and then, counterintuitively, increased relative to the medium-sized D variant.

To understand the origin of these patterns, we performed all-atom molecular dynamics (MD) simulations measuring the ion current with peptide variants at varying positions within the MspA constriction. In a typical simulation, a polypeptide chain was threaded through a reduced-length model of the MspA nanopore embedded in a lipid bilayer and surrounded by 0.4 M KCl electrolyte (Fig. 2D). Peptides with either a W or G substitution in a mixed D/E sequence were examined under a +200 mV bias at various locations relative to the MspA constriction (see materials and methods section 6 and figs. S5 to S8 for details). Patterns of ionic current blockades resulted in Fig. 2E (top panel), matching the counterintuitive blockade current patterns that were experimentally measured for G and W substitutions (compare Fig. 2, A and B). Furthermore, the ion current correlated with the nanopore constriction volume that was available for ion transport near the pore mouth (Fig. 2E, bottom panel), with the latter quantity being more accurately characterized by the all-atom MD method (*19*). In the case of a G residue, its upward motion was accompanied by an increase of the nanopore volume (Fig. 2E, bottom), which subsided as the residue left the nanopore constriction (Fig. 2F), in sync with the blockade current (Fig. 2E, top). A W residue, however, reduced the nanopore constriction volume when it was located below the constriction (Fig. 2E, top) but increased the volume at and above the constriction. The latter counterintuitive effect could be traced back to a binding of the W side chain to the nanopore surface above the constriction (Fig. 2G). Thus, a glycine substitution merely increases the nanopore volume as the residue passes through the constriction, whereas the tryptophan residue decreases the volume when its side chain enters the constriction and subsequently

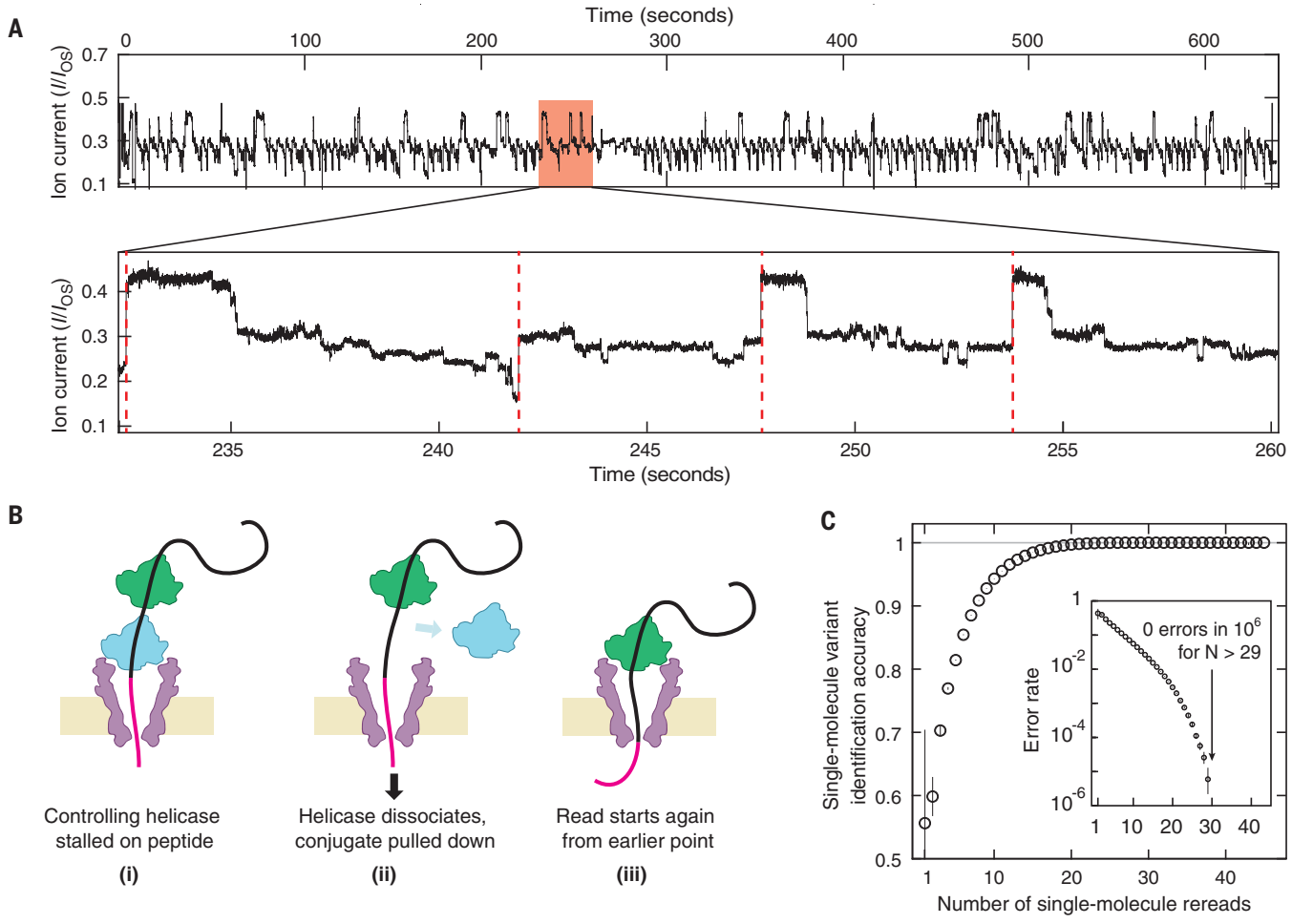

Fig. 3. Rereading of a single peptide. (**A**) Highly repetitive ion current signal corresponding to numerous rereads of the same section of an individual peptide (in this case, the G-substituted variant). The expanded plot (bottom) shows a region that contains four rewinding events (red dashed lines), where the trace jumps back to level 52 ± 2 of the consensus displayed in Fig. 2A. (**B**) Rereading is facilitated by helicase queueing, where (i) a second helicase binds behind the primary helicase that controls the DNA-peptide conjugate, rereading starts when (ii) the primary helicase dissociates, and (iii) the secondary one becomes the primary helicase that drives a new round of reading. (**C**) By using information from multiple rereads of the same peptide, the identification accuracy can be raised to very high levels of fidelity. These results indicate that with sufficient numbers of rereads, random error can be eliminated and single-molecule error rate can be pushed lower than 1 in 10^6 even with poor single-pass accuracy. Inset is a logarithmic plot of the error rate = 1 − accuracy.

increases the volume when its side chain binds to the inner nanopore surface (fig. S9).

To quantitatively assess the distinguishability of peptide variants, we computed a so-called confusion matrix (Fig. 2C). Using a hidden Markov model, we quantified the relative likelihoods of the alignments to the three consensus sequences for 119 reads withheld from the consensus sequence generation, finding that we could identify the correct variant with an average accuracy of 87% (materials and methods section 7). This high rate of correct single substitution identification compares favorably to early nanopore experiments, which identified single-nucleotide variants with considerably lower accuracy (*17*). Still, the limited single-read accuracy is an ongoing challenge in developing nanopore sequence analysis approaches, requiring the implementation of strategies to increase sequencing fidelity to acceptable levels (*18*, *20*). The largest error modes in nanopore reads are due to random effects, as enzymes step stochastically both forward and backward and sometimes step too quickly to be clearly resolved, resulting in incorrect step identifications. In DNA sequencers, this random error is typically addressed by obtaining 20× coverage or more, averaging many independent reads of different molecules. However, for a truly single-molecule technology, single-read accuracy is essential.

The identification fidelity of our nanopore protein reader can be greatly increased by obtaining many independent rereadings of the same individual molecule with a succession of controlling helicases, eliminating the random errors that lead to inaccuracies in nanopore reads. At a very high concentration of helicase, on the order of 1 μM, the DNA in the pore nearly always had a second helicase queued up behind the one controlling its motion (Fig. 3B) (*21*). When the first helicase reached the linker at the end of the DNA section, it could no longer process the molecule and subsequently fell off. The DNA-peptide conjugate was then immediately pulled back into the nanopore such that the queued helicase, which was still bound to the DNA, took control as the new DNA-pulling enzyme. This "rewound" the system and initiated a new and independent read of the peptide. The numbers of rereads on the same single peptide can be very large: Fig. 3A shows an example of a raw data trace with 117 rereads on a single peptide containing the G substitution. This event was purposefully ended by the reversal of voltage to eject the DNA-peptide conjugate from the pore. We observed a typical rewinding distance of ~17 helicase steps, commensurate with a rewinding by a distance of ~17 amino acids, a number that is consistent with the roughly nine DNA bases that are bound within the controlling helicase (*16*). Of the 117 rereads in

Fig. 3A, 45 rereads stepped back far enough to provide a reread of the variant site.

We observed significant improvement of the read accuracy with an increasing number of rereads (Fig. 3C). To quantify the increase in the accuracy of the readings as a function of the number of rereadings, we randomly chose subsets of the 45 measured rereads and computed the identification accuracy using N rereads as the fraction of subsets containing N rereads that yielded the correct consensus identification (materials and methods section 8). Even when single reads were limited to as low as ~50% identification accuracy owing to only partial coverage of the variant site, the rereading method allowed single molecules to be identified at high levels of confidence. As the inset in Fig. 3C shows, the error rate decreased with the number of rereads, yielding an undetectably low error rate (<1 in 10^6) when using more than ~30 rereads of an individual peptide. Analysis on reread traces from other variants yielded similar results (fig. S10).

The method described here provides an approach for reading single proteins with sensitivity to single–amino acid changes, which is particularly powerful because of the rereading mode of operation that reduces the stochastic error. Transforming this method into a technology capable of de novo protein sequencing remains a substantial challenge. With any of the 20 amino acids at each position along the protein sequence and a read-head width (*17*) of about eight amino acids, the number of measurements required to build an ion current–to–amino acid map is impractically large. However, many proteomics applications do not require de novo sequencing, instead using other forms of sequence analysis that rely on a priori knowledge of candidate sequences before decoding. These include identifying or "fingerprinting" proteins even in heterogeneous mixtures, mapping posttranslational modifications, and measurements of small samples, all of which involve comparing single-molecule measurements to reference signals of known proteins and interesting variants.

Our methodology has several limitations, but these may be addressed experimentally. Although the pore is capable of translocating heterogeneously charged peptides with neutral polar, nonpolar, negative, and positive amino acids (supplementary text section 1; sample reads shown in fig. S11), highly positively charged peptides may not be efficiently translocated through the pore. Fortunately, analysis of the human proteome reveals that negatively charged stretches of protein sequence are more common than positively charged stretches (*22*), particularly in alkaline pH conditions like those used in our experiments. If needed, the MspA pore can be engineered to provide stronger electro-osmotic forces, which can exceed electrophoretic forces and translocate analytes regardless of charge (*7*, *23*). The read length intrinsic to the technique, ~25 amino acids depending on the length of the DNA-peptide linker, does allow application of this method to many biologically relevant short peptides, such as 8 to 12–amino acid major histocompatibility complex–binding peptides (*24*). Additionally, this finite read length still represents an improvement over the <10 amino acid–long peptide fragments used in mass spectrometry (*25*), and protein fragmentation and shotgun sequencing methods similar to those used in traditional protein sequencing can naturally be applied to this newly developed technique. Technical modifications such as using a variable-voltage control scheme (*18*) have been shown to improve the accuracy of DNA sequencing, and the physical principle that this scheme relies on is equally applicable to peptide sequencing (supplementary text section 2 and fig. S12).

Reads of DNA-peptide conjugates like those presented here could be measured in high throughput with any existing commercially available nanopore sequencing hardware capable of accommodating MspA (e.g., the commercial MinION system) without requiring any reengineering of the device, changing only the sample preparation and data analysis. Furthermore, our methodology retains the features that enabled the success of nanopore DNA sequencing: low overhead cost, physical rather than chemical sensitivity to small changes in single molecules, and the flexibility to be reengineered to target specific applications. Overall, our findings constitute a promising first step toward a low-cost method capable of single-cell proteomics at the ultimate limit of sensitivity to concentration, with a wide range of applications in both fundamental biology and the clinic.

REFERENCES AND NOTES

1. J. A. Alfaro *et al.*, *Nat. Methods* **18**, 604–617 (2021).
2. J. J. Kasianowicz, E. Brandin, D. Branton, D. W. Deamer, *Proc. Natl. Acad. Sci. U.S.A.* **93**, 13770–13773 (1996).
3. D. Deamer, M. Akeson, D. Branton, *Nat. Biotechnol.* **34**, 518–524 (2016).
4. J. Nivala, D. B. Marks, M. Akeson, *Nat. Biotechnol.* **31**, 247–250 (2013).
5. D. Rodriguez-Larrea, H. Bayley, *Nat. Nanotechnol.* **8**, 288–295 (2013).
6. F. Piguet *et al.*, *Nat. Commun.* **9**, 966 (2018).
7. L. Restrepo-Pérez, C. H. Wong, G. Maglia, C. Dekker, C. Joo, *Nano Lett.* **19**, 7957–7964 (2019).
8. H. Ouldali *et al.*, *Nat. Biotechnol.* **38**, 176–181 (2020).
9. J. Nivala, L. Mulroney, G. Li, J. Schreiber, M. Akeson, *ACS Nano* **8**, 12365–12375 (2014).
10. J. C. Cordova *et al.*, *Cell* **158**, 647–658 (2014).
11. E. A. Manrao *et al.*, *Nat. Biotechnol.* **30**, 349–353 (2012).
12. G. M. Cherf *et al.*, *Nat. Biotechnol.* **30**, 344–348 (2012).
13. I. M. Derrington *et al.*, *Nat. Biotechnol.* **33**, 1073–1075 (2015).
14. S. Yan *et al.*, *Nano Lett.* **21**, 6703–6710 (2021).
15. T. Z. Butler, M. Pavlenok, I. M. Derrington, M. Niederweis, J. H. Gundlach, *Proc. Natl. Acad. Sci. U.S.A.* **105**, 20647–20652 (2008).
16. J. M. Craig *et al.*, *Nucleic Acids Res.* **47**, 2506–2513 (2019).
17. A. H. Laszlo *et al.*, *Nat. Biotechnol.* **32**, 829–833 (2014).
18. M. T. Noakes *et al.*, *Nat. Biotechnol.* **37**, 651–656 (2019).
19. S. Bhattacharya, J. Yoo, A. Aksimentiev, *ACS Nano* **10**, 4644–4651 (2016).
20. A. D. Tyler *et al.*, *Sci. Rep.* **8**, 10931 (2018).
21. A. C. Rand, thesis, University of California, Santa Cruz, Santa Cruz, CA (2017).
22. R. D. Requião *et al.*, *PLOS Comput. Biol.* **13**, e1005549 (2017).
23. D. P. Hoogerheide, P. A. Gurnev, T. K. Rostovtseva, S. M. Bezrukov, *Nanoscale* **9**, 183–192 (2017).
24. M. Wieczorek *et al.*, *Front. Immunol.* **8**, 292 (2017).
25. J. Cox, N. C. Hubner, M. Mann, *J. Am. Soc. Mass Spectrom.* **19**, 1813–1820 (2008).
26. H. Brinkerhoff, A. S. W. Kang, J. Liu, A. Aksimentiev, C. Dekker, Code and Data for "Multiple re-reads of single proteins at single-amino-acid resolution using nanopores," version 1, Zenodo (2021); https://doi.org/10.5281/zenodo.5506740.

ACKNOWLEDGMENTS

We thank J. Gundlach and his lab members at University of Washington for providing the MspA nanopore and for sharing key pieces of software, and we thank F. Mentzou and X. Shi for assistance with data collection, E. van der Sluis for Hel308 purification, and J. van der Torre for helpful advice on DNA construct preparation. We also acknowledge supercomputer time on the Blue Waters at the University of Illinois at Urbana-Champaign; Expanse at University of California, San Diego; and Frontera at the Texas Advanced Computing Center. **Funding:** Dutch Research Council (NWO) NWO-I680 (SMPS) (C.D.); Dutch Research Council (NWO)/Ministry of Education, Culture and Science (OCW) Gravitation programs NanoFront (C.D.); European Research Council Advanced Grant 883684 (C.D.); European Commission Marie Skłodowska-Curie action Individual Fellowship 897672 (H.B.); European Molecular Biology Organization Short-Term Fellowship 8968 (A.S.W.K); National Institutes of Health grant R21-HG011741 (A.A.); Extreme Science and Engineering Discovery environment allocation MCA05S028 (A.A.); Leadership Resource Allocation MCB20012 on Frontera of the Texas Advanced Computing Center (A.A.). **Author contributions:** H.B. and C.D. conceived of the protein analysis method. H.B. and A.S.W.K. conducted nanopore experiments and analyzed the data. H.B. developed additional analysis code. J.L. and A.A. designed and conducted MD simulations. All authors discussed experimental findings and co-wrote the manuscript. **Competing interests:** TU Delft has filed a patent application (PCT/NL2020/050814) on technologies described herein, with H.B. and C.D. listed as inventors. **Data and materials availability:** All data and custom code used in this paper are available for download online (*26*).

SUPPLEMENTARY MATERIALS

science.org/doi/10.1126/science.abl4381
Materials and Methods
Supplementary Text
Figs. S1 to S13
Table S1
References (*27*–*40*)
MDAR Reproducibility Checklist

View/request a protocol for this paper from *Bio-protocol*.

13 July 2021; accepted 24 October 2021
Published online 4 November 2021
10.1126/science.abl4381

Science

Multiple rereads of single proteins at single–amino acid resolution using nanopores

Henry BrinkerhoffAlbert S. W. KangJingqian LiuAleksei AksimentievCees Dekker

Science, 374 (6574), • DOI: 10.1126/science.abl4381

Reading amino acids by nanopore

Nanopore technology enables sensing of minute chemical changes at the single-molecule level by detecting differences in an ion current as molecules are drawn through a membrane-embedded pore. The sensitivity is sufficient to discriminate between nucleotide bases in nanopore sequencing, and other applications of this technology are promising. Brinkerhoff *et al*. developed a nanopore-based, single-molecule approach in which a protein was sequentially scanned in single-amino-acid steps through the narrow construction of a nanopore, and ion currents were monitored to resolve differences in the amino acid sequence along the peptide backbone (see the Perspective by Boškovi# and Keyser). The peptide reader was capable of reliably detecting single-amino-acid substitutions within individual peptides. An individual protein could be re-read many times, yielding very high read accuracy in variant identification. These proof-of-concept nanopore experiments constitute a promising basis for the development of a single-molecule protein sequencer. —DJ